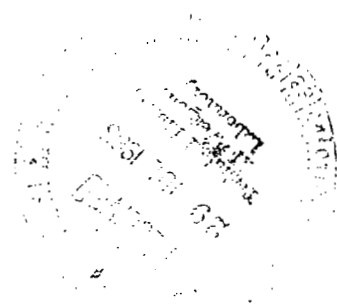**NASA TECHNICAL NOTE**

NASA TN D-4667

NASA TN D-4667

PHOTOGRAPHIC PHOTOMETRY
OF ARTIFICIAL METEORS

by Wendell G. Ayers

Langley Research Center
Langley Station, Hampton, Va.

NATIONAL AERONAUTICS AND SPACE ADMINISTRATION • WASHINGTON, D. C. • JULY 1968

PHOTOGRAPHIC PHOTOMETRY OF ARTIFICIAL METEORS

By Wendell G. Ayers

Langley Research Center
Langley Station, Hampton, Va.

NATIONAL AERONAUTICS AND SPACE ADMINISTRATION

PHOTOGRAPHIC PHOTOMETRY OF ARTIFICIAL METEORS

By Wendell G. Ayers
Langley Research Center

SUMMARY

Two methods of photographic photometry of artificial meteors are presented. These methods relate the amount of radiation that is produced by an artificial meteor in the photographic region of the spectrum to the amount of radiation produced by stars appearing close to the meteor. The relationship is expressed in terms of absolute meteor magnitude. The first method is general and is used when an appreciable difference exists between the structure of the streak image formed by the meteor and of those formed by the stars. The second method is restricted and is used when little difference exists between the structure of the meteor and star images.

INTRODUCTION

Most of the detailed knowledge of the physical processes associated with meteors has been based upon photographic observations of meteors. Using specially designed cameras and high-speed photographic emulsions, meteor astronomers have photographed meteors as dim as fifth-magnitude stars. Photographs of a meteor contain a wealth of quantitative information about the meteor and its origin. The position, velocity, and deceleration of the meteor as well as the amount of light that it produces can be determined photographically. From these basic observable quantities, meteor physicists can deduce a great deal about the physical structure and origin of the object creating the meteor.

A basic interest in the physics of meteors has led to a joint effort between NASA Langley Research Center and the Smithsonian Astrophysical Observatory to conduct a series of artificial-meteor experiments. These meteors were produced by the reentrance of particles of known mass and chemical composition into the earth's atmosphere at altitudes and velocities associated with natural meteors. The purpose of this paper is to describe the data-reduction methods currently employed at the Langley Research Center to determine the amount of radiation produced by these artificial meteors in the photographic region of the spectrum. These methods are an adaptation and extension of methods previously developed for natural-meteor photography.

Two methods of data reduction currently being used for meteor photometry are described. The first method is applied when an appreciable difference exists between the structure of the streak image formed by a meteor and the structure of the streak images formed by the stars on the same photographic plate. The second method is applied when little difference exists between the structure of the meteor and the star images. The second method is an abbreviated form of the first and requires considerably less time and effort for data reduction.

SYMBOLS

A	camera-aperture area, millimeters^2
A'	optical-image area, millimeters^2
a,b	general constants
D	optical density
d	distance along meteor trail in object space, kilometers
E	exposure, joules/meter^2
E_0	exposure for a zero-magnitude star
$e(x_1,y)$	shape function for the trailed images
f	focal length of camera, millimeters
GHA_γ	Greenwich hour angle of Aries, hours-minutes-seconds
H	effective irradiance, watts/meter^2
H_0	effective irradiance of a zero-magnitude star, watts/meter^2
H'	effective irradiance in image space, watts/meter^2
$\overline{H}(\lambda)$	spectral irradiance, watts/meter^2-micrometer
M	absolute meteor magnitude

M_a	apparent stellar magnitude
M_0	initial meteor magnitude (before correction); also, corrected catalog magnitudes of comparison stars
Q	point on the film plane
R	slant range from the camera to the meteor, kilometers
S	ratio of the shutter open time to the total period of operation of the shutter
T	transmittance
$T(\lambda)$	spectral transmittance of atmosphere
t	time, seconds
U	total effective energy per unit path length, joules/meter
U_p	total effective energy per unit path length producing a measurable response in the photographic emulsion, joules/meter
V	velocity in object space, kilometers/second
V'	velocity in image space, millimeters/second
W	trail width, millimeters
x,y	Cartesian coordinates fixed in the image plane, millimeters
x',y'	Cartesian coordinates fixed with respect to the image, millimeters
z	zenith angle, degrees
α	right ascension, degrees
δ	declination, degrees
$\Theta(\lambda)$	spectral transmittance of lens system

3

θ	longitude of optical station, degrees
λ	wavelength, micrometers
λ,μ,ν	direction cosines
σ	camera field angle, degrees
τ	optical-thickness coefficient
$\Phi(\lambda)$	relative spectral response of photographic emulsion
ϕ	latitude of optical station, degrees

Subscripts:

c	camera shutter
cat	catalog
ci	color index
i	points along meteor trail
m	meteor
max	maximum value
PC	plate center
R	slant range
rel	relative values
r	reciprocity-law failure
s	star
T	meteor trail

4

| TC | meteor trail center |

| v | velocity |

| z | zenith angle |

| σ | camera field angle |

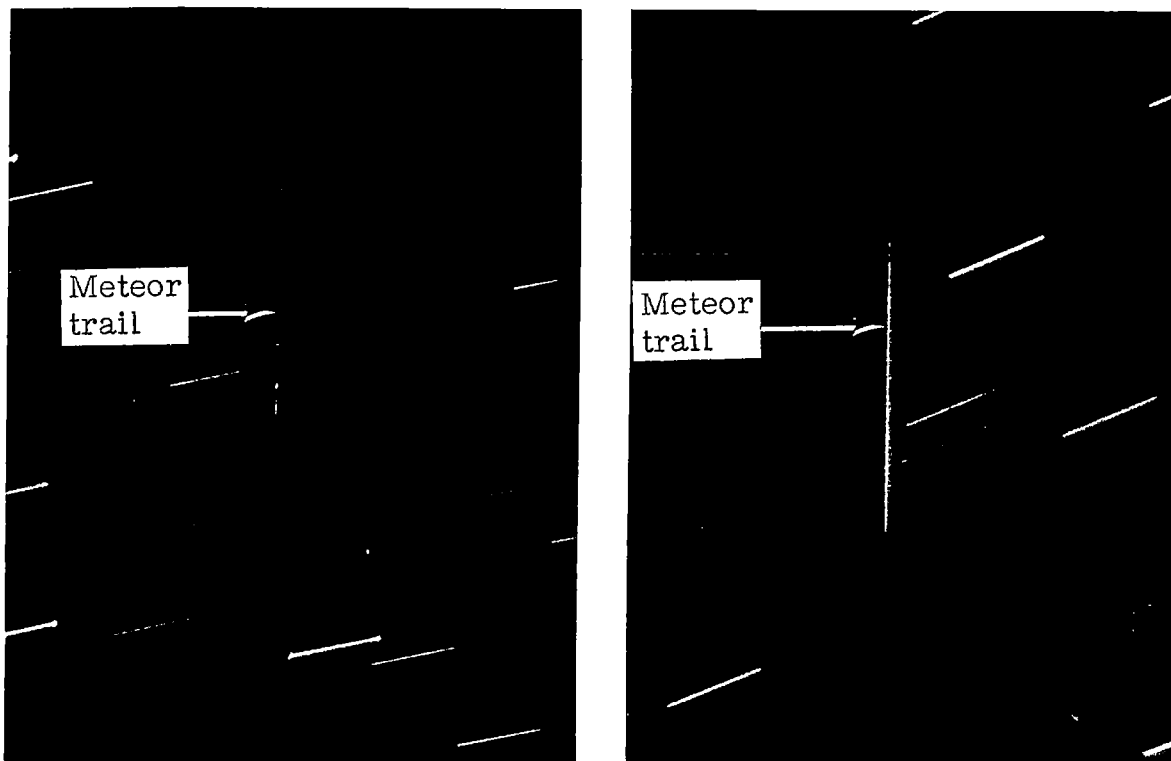| 1/2 | half-exposure point |

DEFINITION OF THE PROBLEM

The methods herein of determining meteor magnitudes are based on a comparison of the trailed image of a meteor with the trailed images of stars appearing close to the meteor trail in a photograph. Photographs of artificial meteors are obtained by fixed ground-based cameras whose shutters are opened before the meteor event and closed after the event. The time during which the shutters are open is usually on the order of 2 or 3 minutes. During this time the star images advance across the photographic plate because of diurnal motion, and produce short streak images. The meteor image also moves across the plate but at a far greater velocity than that of the stars. Consequently, the meteor produces a streak image that is usually longer than the stellar images.

Enlarged portions of two photographs of a typical artificial meteor are shown in figure 1. These photographs were taken from two optical stations, A and B, which were separated by approximately 100 kilometers. The meteor appeared near the center of the photograph taken from station A, and both the meteor and stars appeared in good focus. The meteor appeared near the edge of the photograph taken from station B, and the focus of the meteor was not as good as that of the nearby stars. This difference was probably due to optical abberations in the lens system or the atmosphere. Figure 2 gives the energy distribution across the images of the meteor trails shown in figure 1 at the point of maximum light. The energy distribution across a typical-star image from each photograph is presented for comparison.

Development of a mathematical expression relating the apparent magnitude of a point on the meteor trail to quantities associated with the trailed image of the meteor and with the trailed image of a nearby comparison star of known magnitude is now presented.

An apparent stellar-magnitude scale is defined by the relationship, which can be obtained from page 57 of reference 1

$$M_a = -2.5 \log H/H_0 \tag{1}$$

5

The quantity H/H_0 in equation (1) is the ratio of the effective irradiance at the front aperture of the detection system to the effective irradiance of a zero-magnitude source. The term "effective irradiance" is used to describe radiation that is incident upon the front aperture of a detection system and has the potential of producing a measurable response in the detector.

The effective irradiance from a star or meteor for a photographic system may be described mathematically in the following manner:

Let the spectral irradiance $\overline{H}(\lambda)$ be the radiant power per unit area in the wavelength interval λ to $(\lambda + d\lambda)$ that would be incident upon the front aperture of the camera if the intervening media between the aperture and the radiating source were perfectly transparent. Let $T(\lambda)$ be the transmittance of the intervening media; $\Theta(\lambda)$, the transmittance of the optical system; and $\Phi(\lambda)$, the relative response of the photographic emulsion in the wavelength interval λ to $(\lambda + d\lambda)$. The irradiance at the front aperture of the camera potentially effective in producing a photographic response is given by the expression

$$H = \int_0^\infty T(\lambda)\Theta(\lambda)\Phi(\lambda)\overline{H}(\lambda)d\lambda \qquad (2)$$

Whether or not H will produce a measurable photographic response depends upon many factors including the intensity of the source and the overall sensitivity of the photographic system.
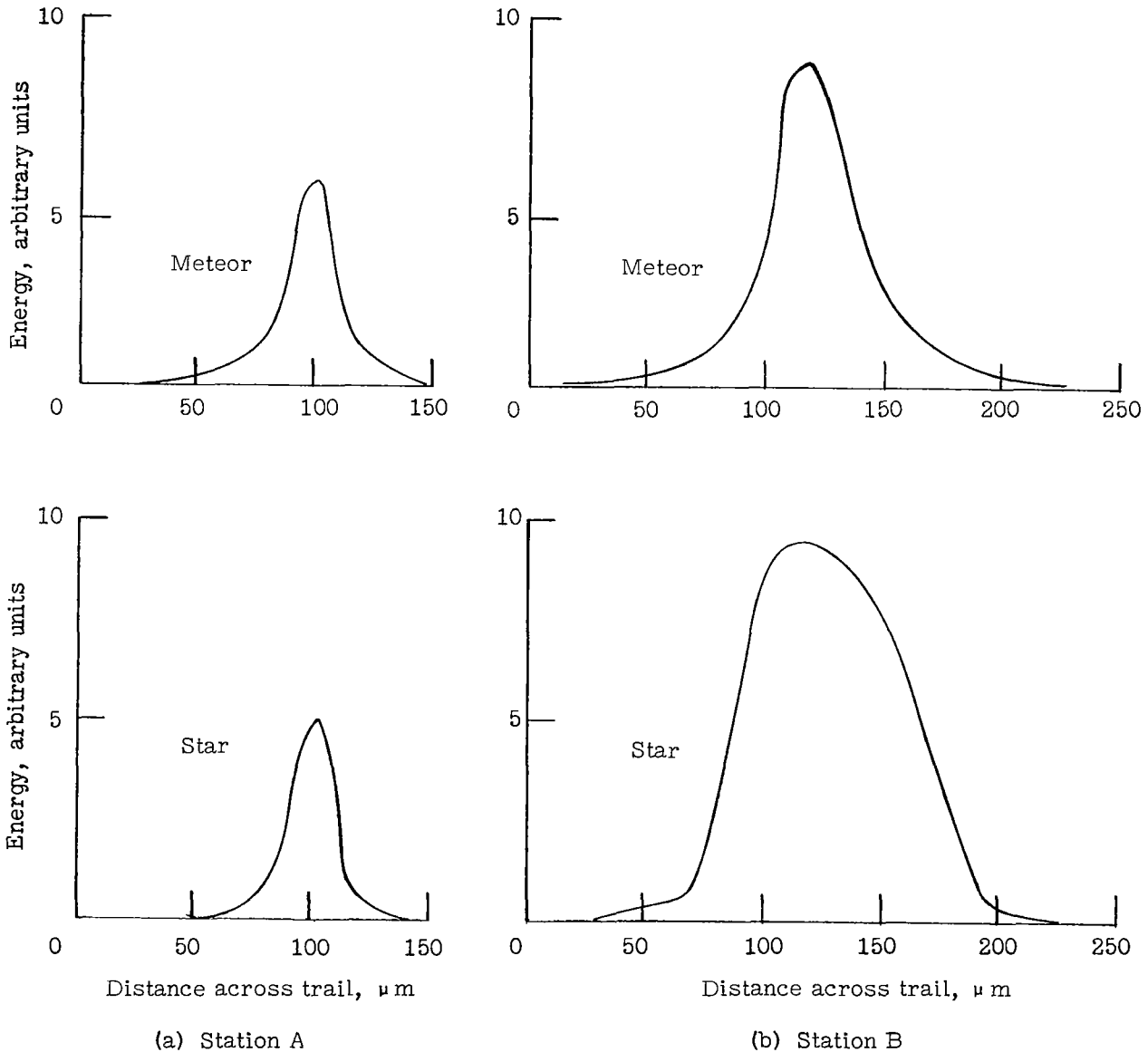

(a) Station A   (b) Station B

Figure 2.- Energy distribution across the images of the meteor trails shown in figure 1 and across typical star-image trails from the respective photographs.

Consider the phenomenon of radiant energy, emitted by a distant source such as a meteor or star, incident upon the front aperture of a camera, and brought to focus on a photographic emulsion. Let the camera-aperture area be A and the image area be A'. From the principle of conservation of energy

$$\int_A H \, dA = \int_{A'} H' \, dA' \tag{3}$$

where H' is the effective irradiance due to the source in the image plane. The size and shape of the image and the distribution of the radiant flux within the image depend upon the spatial extent of the source and the imaging properties of the complete optical system.

If H is constant over A, then

$$H = \frac{1}{A} \int_{A'} H' \, dA' \tag{4}$$

Figure 3.- Schematic representation of optical image moving along x-axis.

If the source moves relative to the camera, the image of the source will move with some velocity V', in the film plane. Let the direction of motion of the image be along the x-axis of a coordinate system fixed in the film plane and consider an elemental area, dx dy, at the point $Q(x_1, y_1)$ on the film plane and in the path of the moving image. (See fig. 3.) The photographic exposure at Q due to the moving image is

$$E(x_1, y_1) = \int H'(x_1, y_1, t) \, dt \tag{5}$$

with the limits of the integral set by the length of time that it takes the image to traverse the elemental area dx dy.
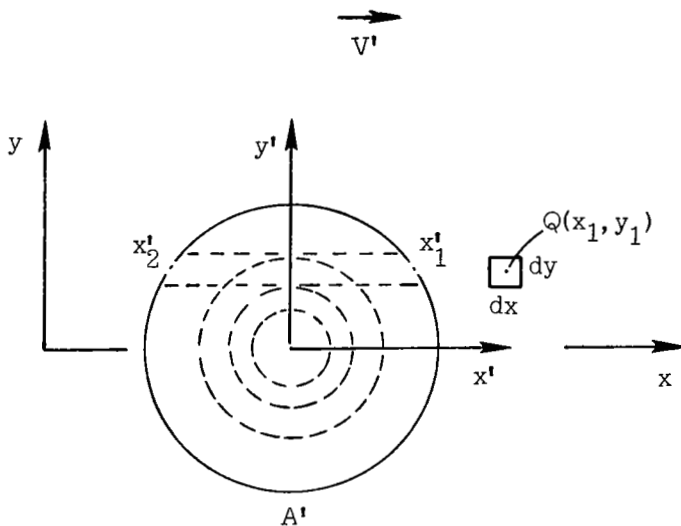
Assume that H' and V' are constant with respect to time in the time interval that it takes the image to traverse dx dy, and take a coordinate system fixed with respect to the image so that

$$\left.\begin{array}{l} x' = x - V't \\ y' = y \end{array}\right\} \tag{6}$$

The exposure at Q then becomes

$$E\left(x_1, y_1\right) = \frac{1}{V'} \int_{x_2'}^{x_1'} H'\left(x_1, y_1, x'\right) dx' \tag{7}$$

According to equation (7), the exposure at the point Q is proportional to the integral of the radiant flux contained in the area $\left(x_1' - x_2'\right) dy$. The complete evaluation of the integral in equation (4) is obtained by the operation

$$U\left(x_1\right) = \int E\left(x_1, y\right) dy \tag{8}$$

with the integration taken over the lateral extent of the image. Equation (8) is an expression for the total effective energy per unit path length at the point x_1 along the image trail.

From equations (1), (4), and (8), the apparent magnitude of a meteor becomes

$$M_{a,m} = M_{a,s} - 2.5 \log \frac{V_m' U_m}{V_s' U_s} \tag{9}$$

The subscript m refers to the meteor and the subscript s refers to the comparison star. Equation (9) relates the apparent magnitude of the meteor to properties of the meteor and of comparison-star images which can be determined by appropriate data-reduction techniques.

TWO METHODS OF PHOTOMETRY

For the purpose of this analysis, a photographic negative containing a meteor trail is assumed to contain trailed comparison-star images and a photometric gray scale relating exposure to photographic transmittance. It is further assumed that the photographic negatives are measured with a microphotometer and that the geometric

parameters of the meteor and comparison stars have been determined by data reduction such as that described in reference 2.

The following list gives the auxiliary information needed in the photometric data-reduction process:

(1) Data from comparison stars should include catalog magnitude, color class, right ascension, declination, color index, trailing velocity, effective exposure time, zenith angle at the time of exposure, and angular distance from the plate center.

(2) Data from the meteor trail should include trailing velocity, effective exposure time, zenith angle at the time of exposure, angular distance from the plate center, and slant range of the meteor from the camera.

Flow charts outlining the data-reduction cycles for both the general and the restricted methods of photometry are shown in figures 4 and 5, respectively. Micro-photometer traces of the meteor and star images are the primary inputs into the cycles. Auxiliary information from several sources is used to transform these traces into values of irradiance from points along the meteor trail. The end product of the cycle is a light curve for the meteor that is expressed in terms of absolute meteor magnitude as a function of time.

The absolute magnitude of a point on a meteor trail is defined as the apparent stellar magnitude of the point if the meteor is at a range of 100 kilometers from the observer and at the zenith. In this definition the stellar-magnitude scale to which the meteor is referred is assumed to be based upon the same detection system as the system used to detect the meteor.

GENERAL METHOD

Selection of Comparison Stars

The first step in the data-reduction procedure is the selection of enough comparison stars from the photographic plate to form a calibration curve. The selected stars are identified on star charts such as those of reference 3, and approximate values of right ascension α and declination δ are determined for each star. The approximate values of α and δ are used to identify the stars in Boss' general catalog of stars (ref. 4), which lists values of α and δ for the year 1950, as well as spectral type and visual magnitudes for stars up to a 7.5 magnitude.

The following rules are used as a guide in the selection of the comparison stars:

(1) Choose enough stars to establish a smooth calibration curve over the dynamic range of the photographic emulsion. Twenty to thirty stars are usually needed to provide this curve.
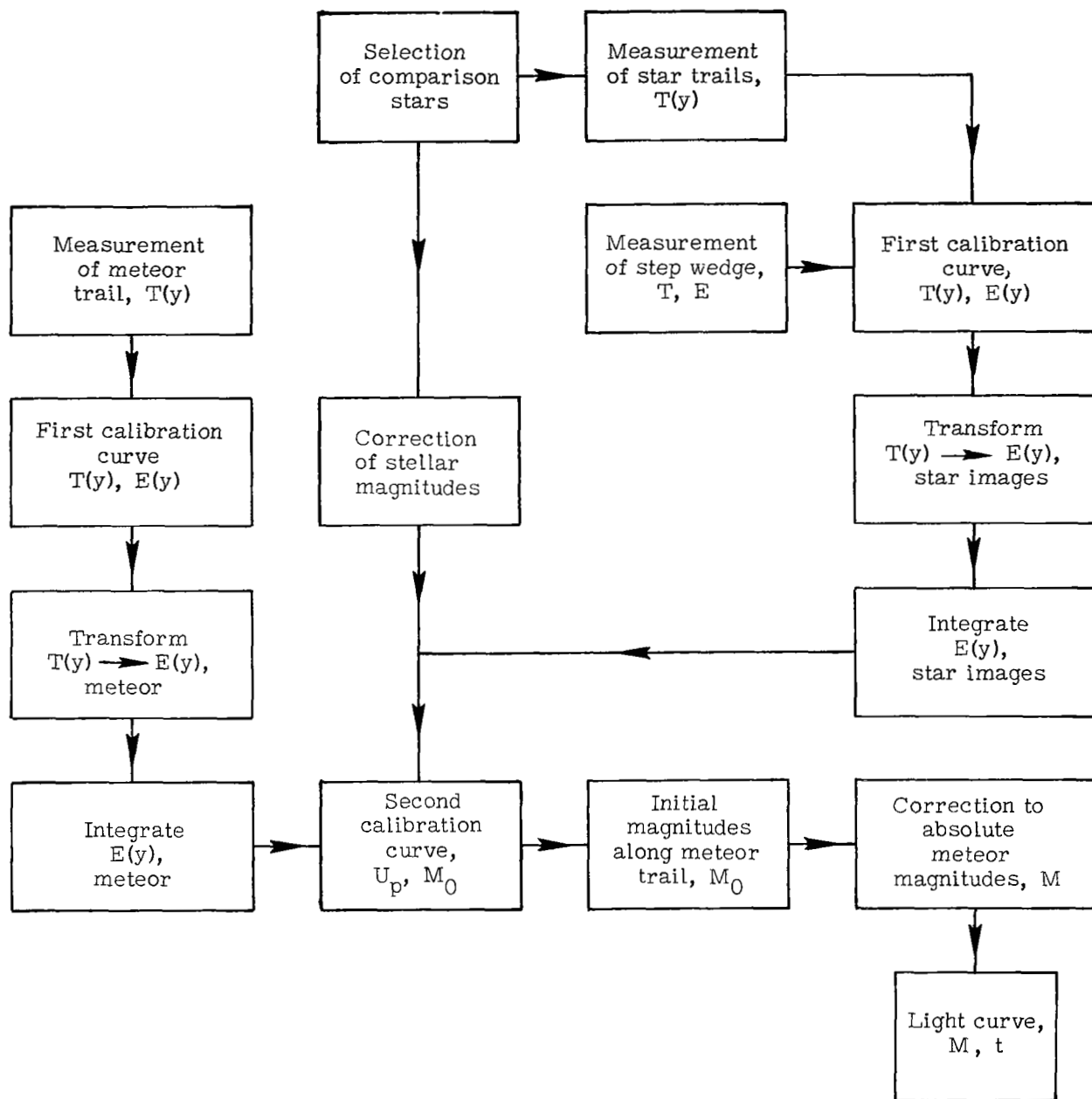
10

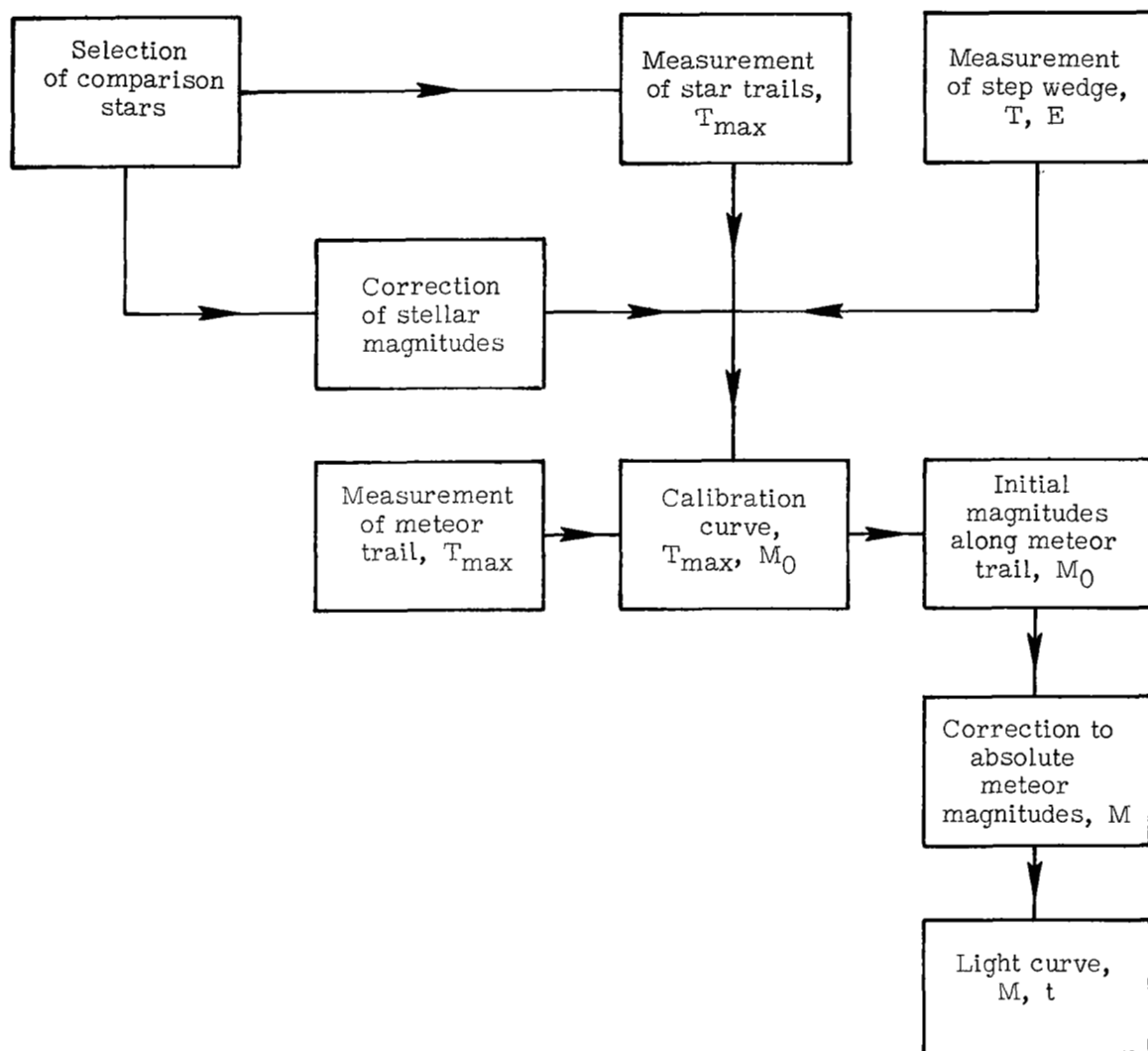Figure 4.- Flow diagram for general method of data reduction.

Figure 5.- Flow diagram for restricted method of data reduction.

(2) Select as the first choice for a star of a particular magnitude the star closest to the center of the meteor trail and closest to spectral type A_0.

(3) Reject double stars, variable stars, and stars of unlisted spectral type.

(4) Reject stars of spectral types outside of the interval B_5 through F_5.

(5) Reject those stars that have magnitudes listed to only one decimal place.

First Calibration Curve

The second step in the data-reduction procedure is to construct a calibration curve for the response of the photographic emulsion to known increments of exposure. These

data are obtained from a sensitometric "step wedge" printed on the photographic emulsion prior to development. The calibration curve defines the nonlinearity of the emulsion with respect to exposure (input) and transmittance (output), and is used to remove the nonlinearity of the microphotometer traces of the calibration stars and the meteor trail. A point-to-point transformation of the microphotometer traces from values of transmittance to values of exposure removes this nonlinearity. An illustration of this transformation is shown in figure 6.
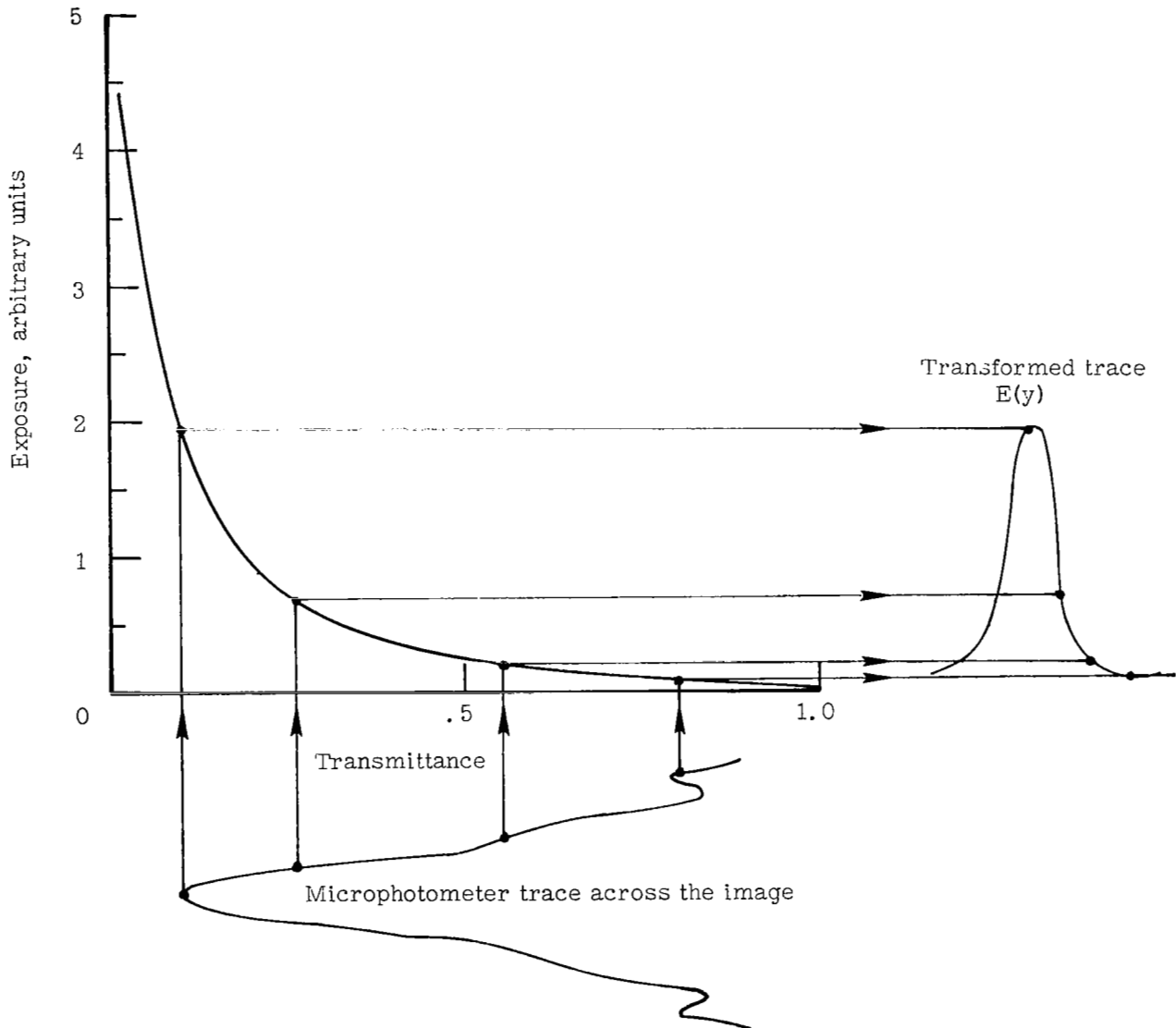

Figure 6.- Schematic representation of the transformation of transmittance values to exposure values.

Second Calibration Curve

The third step in the data-reduction process is to integrate the transformed micro-photometer traces and to form a second calibration curve relating the values obtained from the integrations to stellar magnitudes. In order to obtain this curve a number of corrections must be applied to the catalog values of stellar magnitudes to minimize the differences in apparent magnitude due to the position of the stars on the photographic plate. A convenient approach is to transpose all the comparison stars to the center of the meteor trail. The advantage to this method is that for stars near the meteor trail the corrections are small and no zenith correction need be applied to the trail in the final determination of absolute meteor magnitude.

The correction equation for the comparison stars can be written as

$$M_{TC} = M_{cat} + \Delta M_z + \Delta M_{v,s} + \Delta M_\sigma + M_{ci} \qquad (10)$$

where M_{cat} is the catalog magnitude of the star; ΔM_z is a correction for the difference in zenith angle between the star and the trail center; $\Delta M_{v,s}$ is a correction for the difference between the trailing velocity of the star and the trailing velocity of a star at the center of the meteor trail; ΔM_σ is a correction for the difference between the angular distance of the star from the plate center and the distance of the center of the trail from the plate center; ΔM_{ci} is a color-index correction to transform the visual magnitudes listed in the Boss Catalog (ref. 4) to photographic magnitudes.

These corrections are obtained in the following manner:

(1) The zenith-angle correction ΔM_z is based on a plane-parallel model of the atmosphere as described in reference 1, page 93. For zenith angles less than 75°, ΔM_z is calculated from the equation

$$\Delta M_z = \tau \left(\sec z - \sec z_{TC} \right) \qquad (11)$$

where z is the zenith angle of the star, and z_{TC} is the zenith angle of the meteor trail center. The optical-thickness coefficient τ depends upon the spectral transmittance of the atmosphere. A plot of τ as a function of wavelength is shown in figure 7. Data for this plot were taken from table 3-2 of reference 1. A value of

$$\tau = 0.30 \qquad (12)$$

is used for blue-sensitive photographic emulsions, and a value of
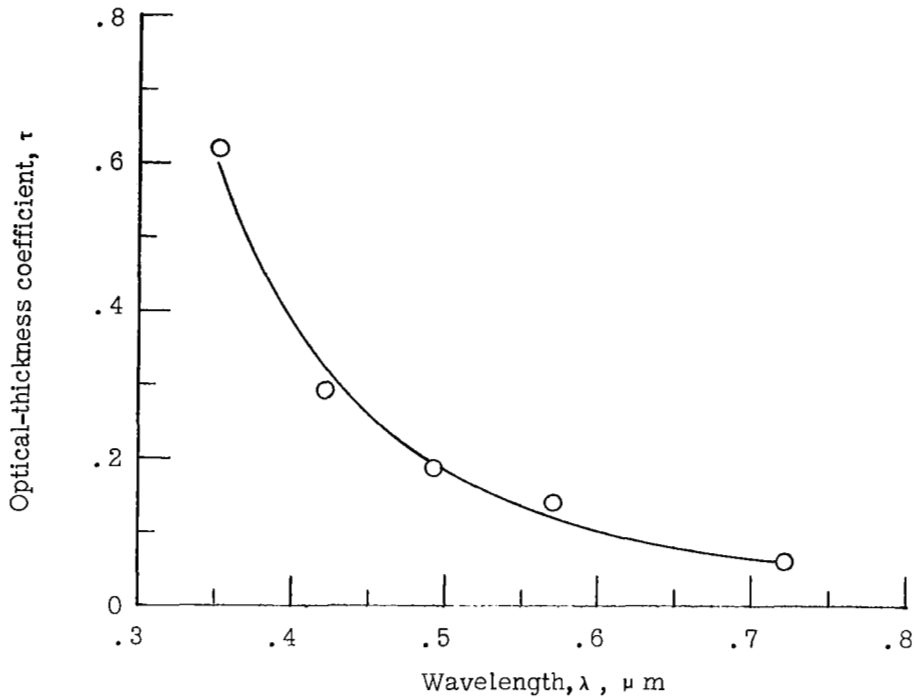
$$\tau = 0.18 \qquad (13)$$

14

Figure 7.- Optical-thickness coefficient for the earth's atmosphere plotted against wavelength.

is used for panchromatic emulsions in the artificial-meteor photometry. Stars at zenith angles greater than 75° are generally not used in the meteor photometry described in this report. Use of such stars would necessitate a correction factor based on empirical methods which would depend upon available data.

The zenith angle of the comparison stars and the trail center may be calculated from the following formula taken from page 242 of reference 5:

$$\text{hav } z = \text{hav } |\phi - \delta| + \cos \delta \cos \phi \text{ hav } t \qquad (14)$$

where

$$t = \theta + \alpha + \text{GHA}_\gamma \qquad (15)$$

The quantities θ and ϕ are assumed to be known. The GHA_γ at the time of the meteor can be obtained from the Air Almanac (ref. 6).

The quantities α and δ may be taken from reference 3 or computed from the following relations:

$$\sin \delta = \nu \qquad (16)$$

15

$$\tan \alpha = \mu/\lambda \tag{17}$$

where λ, μ, and ν are direction cosines in an astronomical equatorial coordinate system computed from the ballistics program described in detail in reference 2.

(2) For the correction ΔM_V, the trailing velocity of a star on a stationary plate in mm/sec is obtained from the formula in reference 7, which (in the notation of the present report) is

$$V'_S = 0.000\ 072\ 92\ f\ \frac{\cos\ \delta}{\cos\ \sigma} \tag{18}$$

It follows that the correction in magnitude due to differences in velocity ΔM_V is given by

$$\Delta M_V = 2.5\ \log\frac{\cos\ \delta}{\cos\ \sigma} - 2.5\ \log\frac{\cos\ \delta_{TC}}{\cos\ \sigma_{TC}} \tag{19}$$

The angular quantities in equation (19) may be computed from geometric data (as given in ref. 2) by the relationships

$$\cos\ \delta = \lambda^2 + \mu^2 = 1 - \nu^2 \tag{20}$$

$$\cos\ \sigma = \lambda\lambda_{PC} + \mu\mu_{PC} + \nu\nu_{PC} \tag{21}$$

(3) The correction ΔM_σ for the difference between the angular distance of the star from the plate center and distance of the center of the trail from the plate center is a function of the optical characteristics of each camera and should be determined experimentally. A representative curve for the off-axis light losses in terms of magnitude for one camera used in the artificial-meteor program is presented in figure 8. The correction is given by

$$\Delta M_\sigma = M_{\sigma,s} - M_{\sigma,TC} \tag{22}$$

(4) The color-index correction ΔM_{ci} is independent of the position of the stars on the photographic plate but is a function of the spectral response of the photographic emulsion and the spectral characteristics of the stars. The color-index correction converts photometric (visual) magnitudes as listed in reference 4 to photographic magnitudes. Figure 9 is a graphical representation of the color index for a blue-sensitive and a panchromatic emulsion. The data for these curves were taken from reference 8.
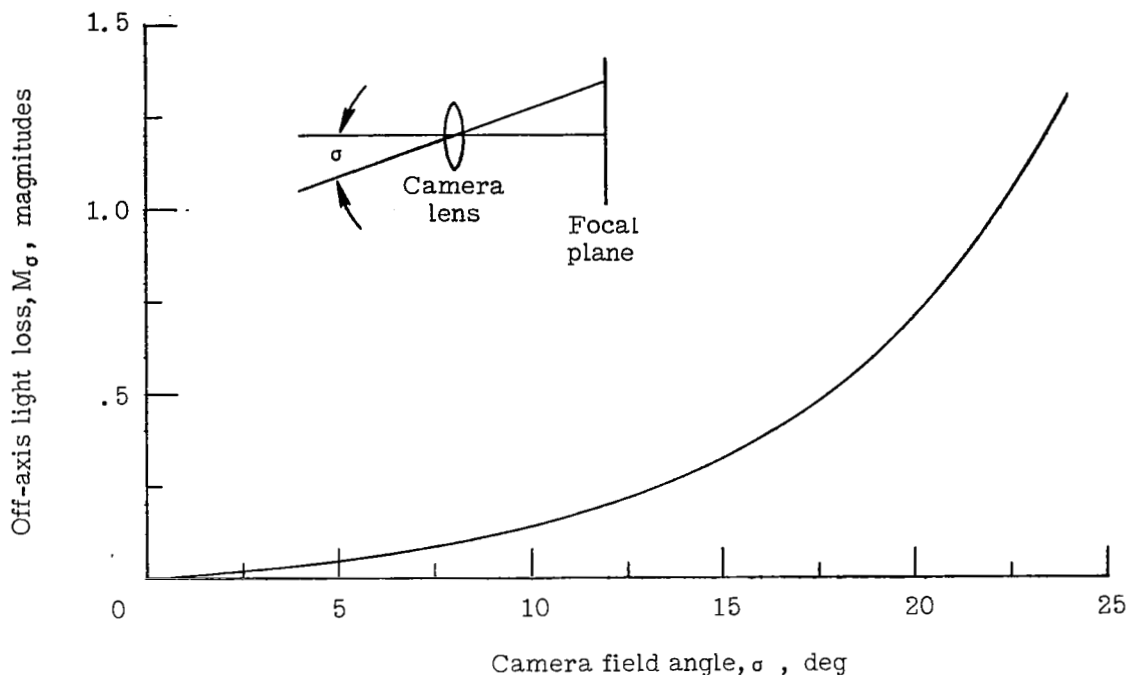
Figure 8.- Off-axis light-loss calibration curve for a typical camera used in the artificial meteor program.

These correction factors are generally small if the comparison stars are chosen close to the meteor trail. The calculation of these correction factors can be time consuming if the procedure is not automated or if graphical methods are not employed. Experience has shown that the correction factors can be ignored if the sum of the corrections for the most extreme cases (usually the comparison stars farthest from the meteor trail) is less than 0.1 magnitude.

Finally, a smooth calibration curve is formed by plotting the stellar-image energy per unit path length that is effective in producing a measurable response in the photographic emulsion against the corrected catalog magnitudes of the stars. A typical calibration curve of this type is shown in figure 10. This curve, in general, will be linear over several stellar magnitudes when plotted in the form presented in figure 10. However, the slope of the straight-line portion of the calibration curve may differ from the slope of the curve given by equation (1) because the calibration points do not include the effective energy below the limits of detectivity of the photographic emulsion.

Determination of Initial Meteor Magnitudes

The fourth step in the data-reduction process is the transformation of the microphotometer traces of the meteor trail to a magnitude scale. This transformation is made by transposing the microphotometer traces of the meteor trail to exposure values,
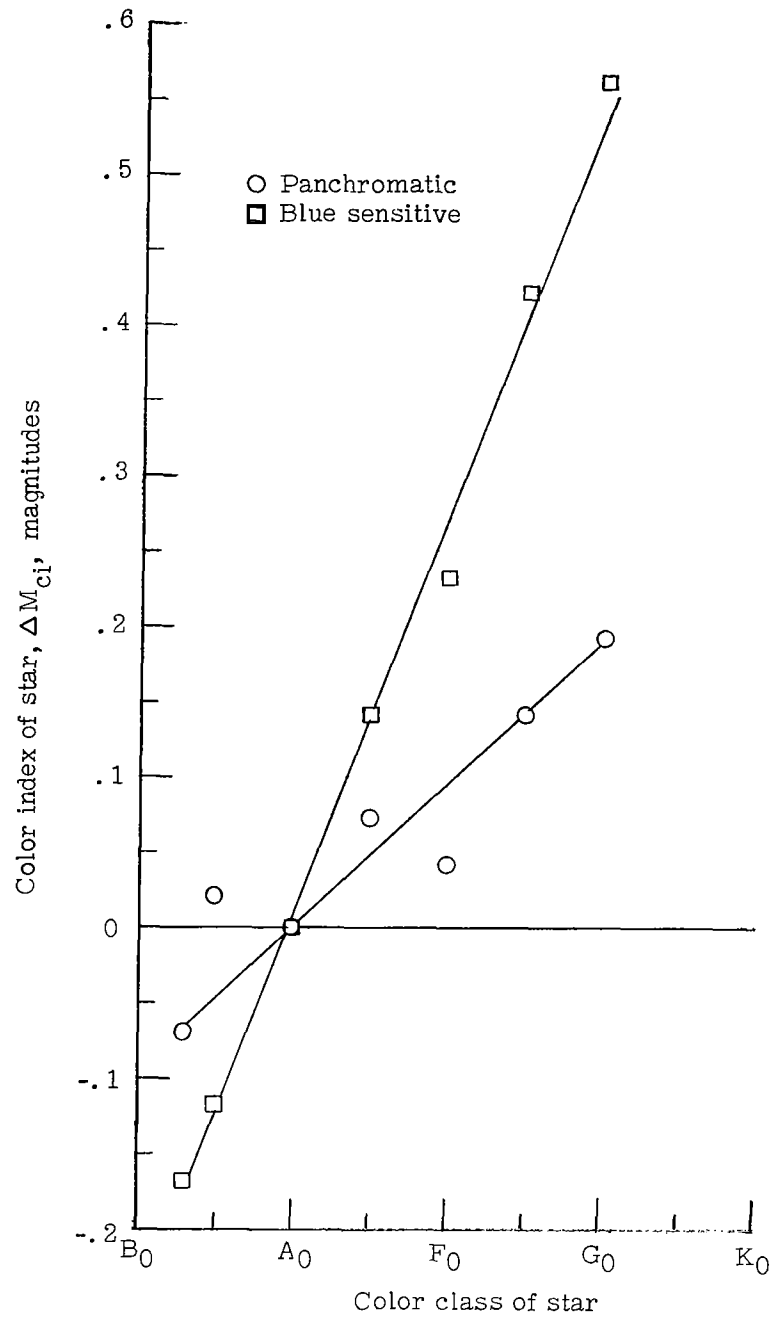
Figure 9.- Graphical representation of the color index for blue-sensitive and panchromatic emulsions.
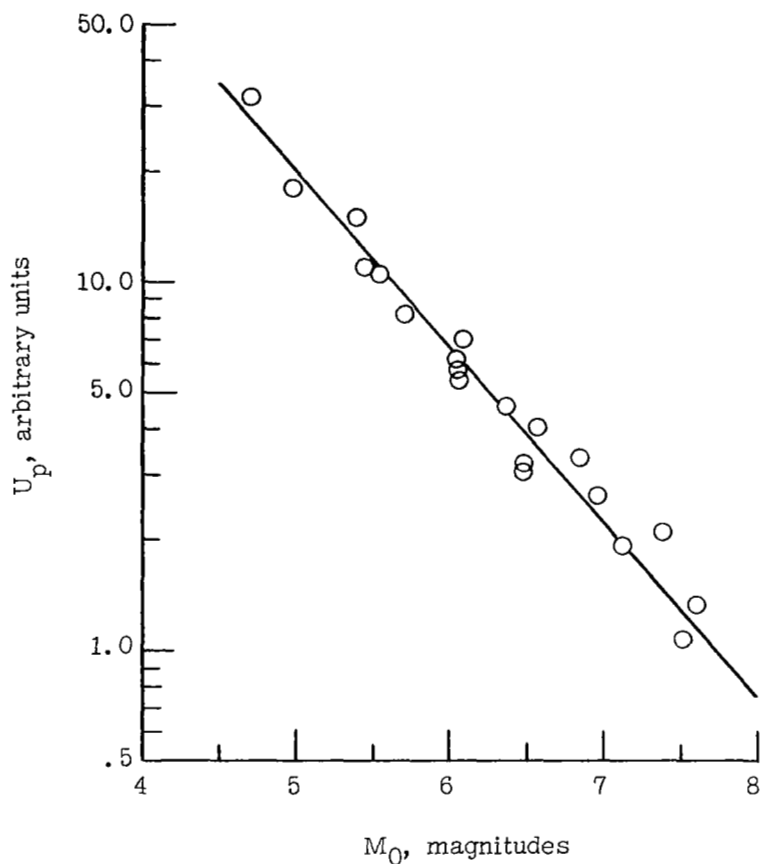
Figure 10.- Typical calibration curve relating the energy per unit path length in the stellar images that is effective in producing a measurable response in the photographic emulsion to the corrected catalog magnitudes of the comparison stars.

integrating under the resulting curves, and comparing these values to the calibration curve to obtain values of initial magnitude at points along the meteor trail. The magnitudes obtained in this manner require several corrections to convert them to absolute meteor magnitudes.

Determination of Absolute Meteor Magnitudes

The fifth step in the data-reduction process is conversion of the values of initial magnitude obtained in step four at points along the meteor trail to values of absolute meteor magnitude. The correction formula used to convert these values of initial magnitudes to values of absolute meteor magnitudes is

$$M = M_0 + \Delta M_{v,m} + \Delta M_r + \Delta M_R + \Delta M_c + \Delta M_T \tag{23}$$

19

where M_0 is the initial magnitude of a point on the meteor trail obtained from the calibration curve; $\Delta M_{v,m}$ is a correction for the difference in trailing velocity of the image of the meteor and the image of a star at the center of the trail; ΔM_r is a correction for reciprocity failure of the photographic emulsion; ΔM_R is a correction for the difference in the range of the meteor and 100 kilometers; ΔM_c is a correction for the differential dimming of the meteor trail and the calibration-star images when a camera with a repeating shutter is used; ΔM_T is a correction for points along the meteor trail to the center of the trail and includes a zenith correction and an off-axis correction. These corrections are obtained in the following manner:

(1) The velocity correction $\Delta M_{v,m}$ is needed to compensate for the difference in effective exposure between the meteor trail and the comparison-star images due to the differences in their trailing velocities on the photographic plate. The correction is given by

$$\Delta M_{v,m} = -2.5 \log \frac{V'_m}{V'_{s,TC}} \tag{24}$$

where V'_m is the trailing velocity of the meteor, and $V'_{s,TC}$ is the trailing velocity of a star at the center of the meteor trail. If the photographic record is from a camera with a repeating shutter such that the meteor trail is broken into several segments of lengths Δx_i, then the average trailing velocity of the meteor at the ith point on the trail is given by

$$\overline{V}_i = \frac{\Delta x_i}{\Delta t} \tag{25}$$

where Δt is the open time of the shutter.

If the photographic record is from a camera for which the shutter was open during the entire time of the meteor event, then

$$\overline{V}_i = \frac{\Delta x_i}{\Delta d_i} V_i \tag{26}$$

where Δd_i is a distance along the meteor trail in object space corresponding to the distance along the trail Δx_i in image space, and V_i is the velocity of the meteor in object space. The quantities in the right-hand members of equations (25) and (26) are obtained from the geometric data.

The velocity of a star at the center of the meteor trail is given by equation (18); however, the focal length of the camera must be known in order to use this equation. If

unknown, the focal length can be computed from the plate constants a_x and b_x in equation (11) of reference 2. In the notation of the reference, the focal length of the camera is given by

$$f = \left(a_x^2 + b_x^2\right)^{1/2} \tag{27}$$

The velocity correction is usually a large correction since the trailing velocity of the meteor is approximately 1000 times the trailing velocity of a calibration star.

(2) Because of the large differences in the effective exposure times of the meteor trail and the star images, failure of the reciprocity law (see p. 132 of ref. 9) for photographic emulsions may play an important role in the determination of meteor magnitudes.

The effects of reciprocity-law failure as it applies to meteor photometry can be determined experimentally or estimated from manufacturer's data. Figure 11 is a plot of the reciprocity-law failure for one of the panchromatic emulsions used in the artificial meteor experiments. The smooth curve was derived from manufacturer's data and represents the average of several measurements. These measurements were obtained from extended stationary sources exposed for definite time intervals. The data points are values obtained from measurements of moving-point sources. The values for the velocity of the moving images have been converted to a time scale by the relationship

$$t = \frac{W_{1/2}}{V'} \tag{28}$$

where $W_{1/2}$ is the width of the image at the half-exposure point. The half-exposure point is defined as the point on the image where the exposure is one-half its maximum
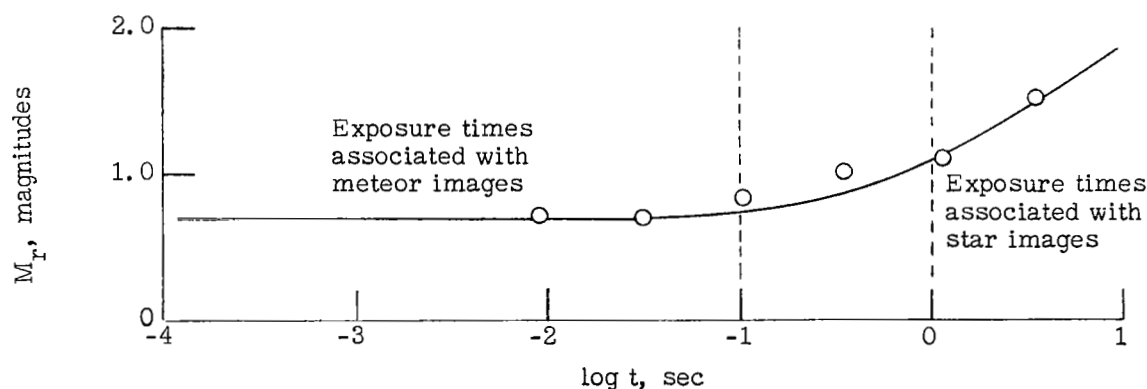

Figure 11.- Calibration curve for the reciprocity-law failure of a high-speed panchromatic emulsion.

value. In this case the image half-width was 50 microns. The reciprocity correction to the meteor data is obtained from a curve of the type shown in figure 11 by

$$\Delta M_r = M_{r,s} - M_{r,m} \tag{29}$$

(3) The range correction ΔM_R is a correction based on the inverse-square law of radiation. This correction is used to normalize all meteors to a common range (100 km) for comparison purposes. The correction is given by

$$\Delta M_R = 10 - 5 \log R \tag{30}$$

where the range R of the meteor from the optical observation station is given in kilometers. Values of R from points along the meteor trail are obtained from the geometric reduction.

(4) The shutter correction ΔM_c is needed only for those photographs made with a camera which uses a repeating shutter. This correction is given by

$$\Delta M_c = -2.5 \log S \tag{31}$$

where S is the ratio of time that the shutter is open during one period of operation to the total time of the period.

(5) The correction ΔM_T for points along the meteor trail relative to the center of the trail is given by

$$\Delta M_T = \Delta M_\sigma + \Delta M_z \tag{32}$$

where ΔM_σ is calculated from equation (22), and ΔM_z is calculated from equation (11).

RESTRICTED METHOD

If the microphotometer traces (see fig. 2) show little difference between the photographic image of the meteor and those of the comparison stars, as in the case of the photograph from station A, then the complete method of photometry can be modified to shorten the data-reduction cycle significantly and to give results that are as accurate as the complete method of photometry.

The integral in equation (8) can be written in the form

$$\int E \, dy = E_{max} \int e\left(x_1, y\right) dy \tag{33}$$

where $e\left(x_1, y\right)$ is the relative shape function for the trailed image. If the relative shape functions are equal for the meteor and the comparison stars, then equation (9) reduces to

$$M_{a,m} = -2.5 \log \frac{V'_m E_{m,max}}{V'_s E_{0,max}} \tag{34}$$

The utility of equation (34) lies in the fact that only maximum values of the microphotometer traces are needed to determine the ratio of irradiance. The lengthy process of transposing the microphotometer traces to exposure values and integrating each transposed curve is eliminated from the data-reduction cycle. (See figs. 4 and 5.) Only one calibration curve between the magnitude of the stars and their values of transmittance at maximum exposure is needed. The number of comparison stars needed to form the calibration curve is also reduced by approximately a factor of three compared to the number of stars needed in the general method of reduction.

Selection of Comparison Stars

The first step in the data-reduction process is the selection of the comparison stars. The selection of comparison stars for the restricted method of photometry generally follows the same procedure as that outlined for the general method of photometry. However, there are two important exceptions:

(1) Only stars whose transmittances at peak exposure lie on the straight-line portion of the calibration curve need be selected.

(2) Approximately 10 stars are all that need to be selected.

Construction of the Calibration Curve

The second step in the data-reduction process is the construction of a calibration curve relating the transmittance at maximum exposure of the stars to their corrected catalog magnitudes. The shape of the calibration curve is determined from measurements of the sensitometric step wedge. A plot of $\log T$ against $-2.5 \log E_{rel}$, where E_{rel} is the value for relative exposure of the step wedge, produces a response curve for the photographic emulsion that is linear over a certain range of exposure. By defining

$$\left.\begin{aligned} D &= -\log T \\ M_0 &= -2.5 \log E_{rel} \end{aligned}\right\} \tag{35}$$

the equation for the straight-line portion of the relative-response curve can be written as

$$M_0 = a - bD \tag{36}$$

where a and b are constants to be determined.

The relative-response curve can be translated to a stellar-magnitude scale determined by the comparison stars by redetermining the constant a. The equation for the straight-line portion of the curve in the new coordinate system becomes

$$M_0 = a_s + bD_{max} \tag{37}$$

where M_0 is the corrected catalog magnitude of the comparison stars, and D_{max} is the value of D for the calibration stars at the point of maximum exposure. The best value for the constant a_s is taken to be the arithmetic mean of the values computed by using each comparison star. The resulting calibration curve is a response curve for the photographic emulsion relating the transmittance at the point of maximum exposure to values of stellar magnitude. A typical calibration curve is shown in figure 12. This calibration curve serves the same purpose as the second calibration curve described in the complete method of photometry.
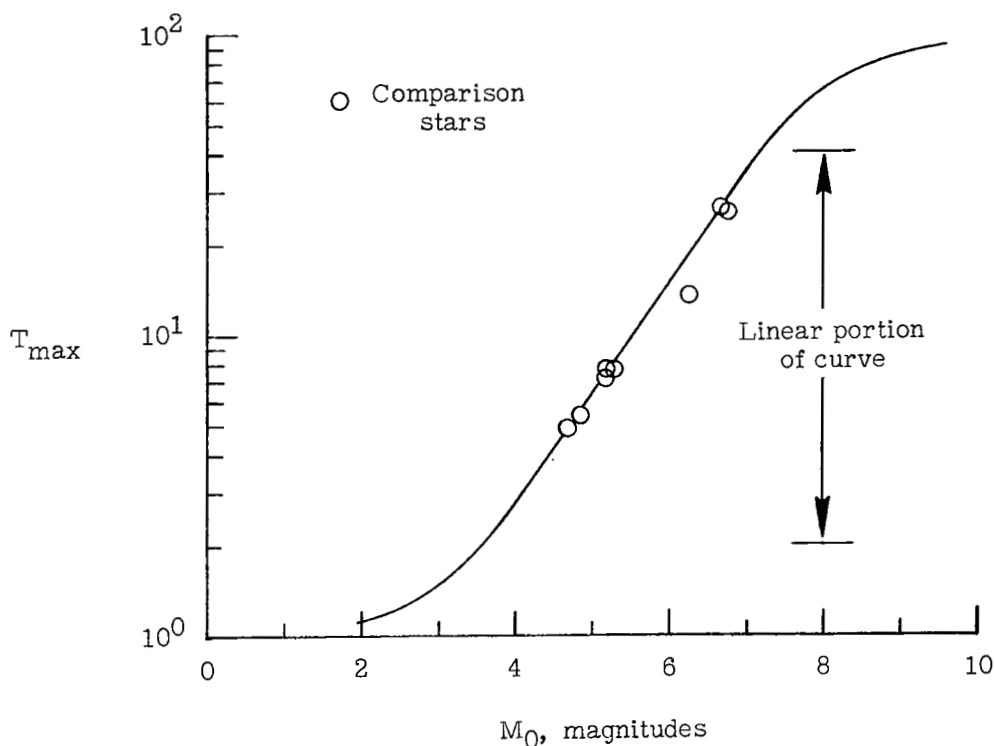

Figure 12.- Typical calibration curve relating the transmittance at maximum exposure to the corrected catalog magnitudes of the comparison stars.

Determination of Initial Meteor Magnitudes

The third step is the transformation of the microphotometer traces of the meteor trail to a magnitude scale. The transformation is made by comparing values of transmittance at the point of maximum exposure of the cross-sectional microphotometer traces of the meteor trail to the calibration curve to obtain corresponding values of magnitude.

Determination of Absolute Meteor Magnitude

The fourth step in the data-reduction process is the conversion of the values of magnitude obtained from the calibration curve for points along the meteor trail to values of absolute meteor magnitude. The conversion is made in exactly the same manner as described in the section dealing with the complete photometry method.

ACCURACY OF THE METHODS

The accuracy of the final light curve depends to a large extent upon the photographic quality of the meteor photograph as well as the accuracy of the measurements and the correction factors that are part of the data-reduction procedures. A complete error analysis of the methods has not been attempted; however, in practice the light curves obtained from well-exposed photographs of a meteor will generally differ by less than 0.2 magnitude over most of the meteor trail, and the agreement in results from photographs taken from different optical stations is of the same order as that obtained from photographs taken from the same optical station.

Light curves for the meteor that is shown in figure 1 are presented in figure 13. The data from station A were reduced by the restricted method of photometry; the data from station B were reduced by the general method.

A question may arise as to which method should be used for a particular reduction. The relative shape function (eq. (33)) of a point on the meteor trail is seldom identical to the relative shape function of a comparison-star image, and the relative shape functions of the comparison-star images are seldom identical to each other. If the distribution of the energy in the meteor image is generally the same as the distribution of the energy in the comparison-star images and if the integral of the relative-shape function of the meteor does not differ by more than 10 percent from that of a typical comparison star, then the restricted method will yield results with the same order of accuracy as the general method.
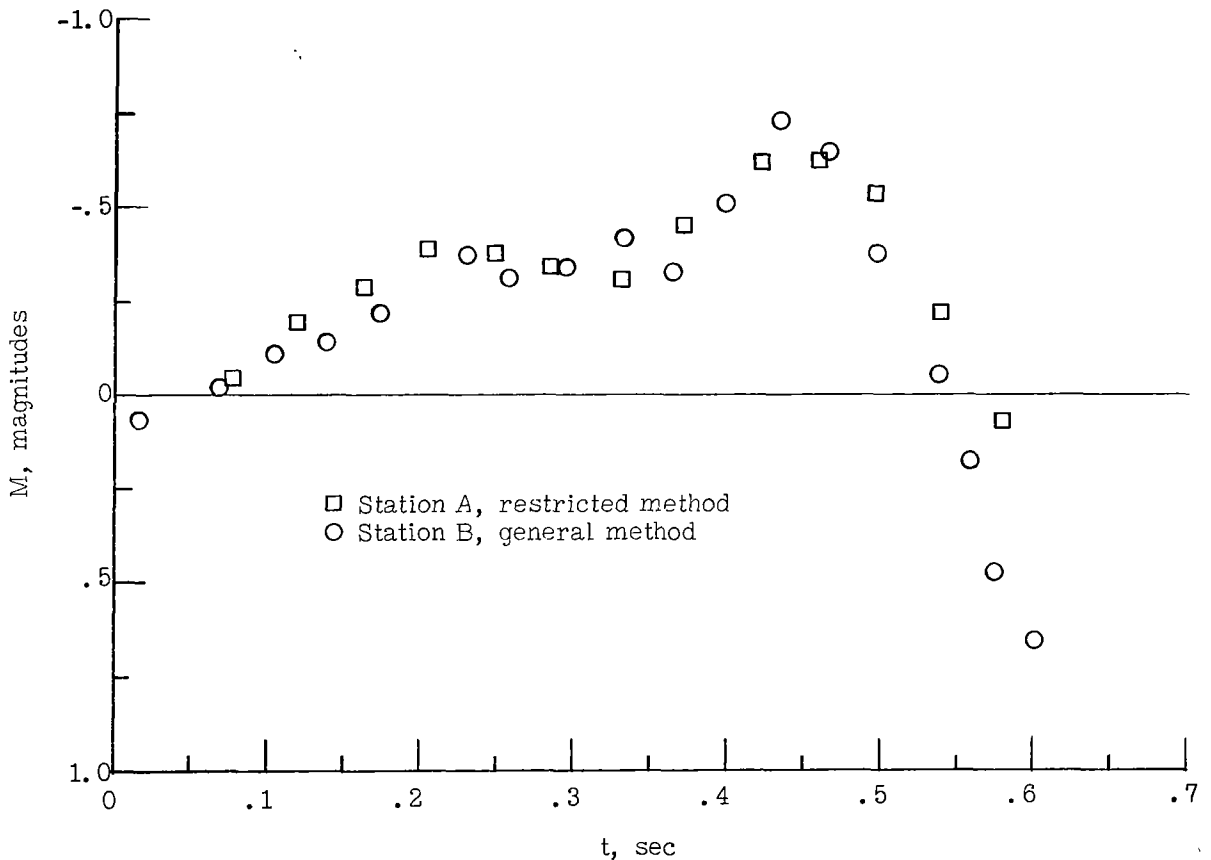
Figure 13.- Light curves for the meteor shown in figure 1. The data from station A were reduced by the restricted method of photometry; the data from station B were reduced by the general method.

CONCLUDING REMARKS

A method of meteor photometry has been presented which takes into account differences between the image structure of a meteor and the image structure of trailed comparison stars. An abbreviated form of this method has also been presented for those cases when little difference in image structure exists. Both methods have been developed in such a manner that many of the factors affecting the photographic effects of the meteor and stars can be isolated and taken into account one by one. This formulation has the advantage that possible sources of error in the determination of the irradiance produced by the meteor can be isolated and identified.

Langley Research Center,
    National Aeronautics and Space Administration,
        Langley Station, Hampton, Va., February 19, 1968,
            709-06-00-01-23.

REFERENCES

1. Blanco, V. M; and McCuskey, S. W.: Basic Physics of the Solar System. Addison-Wesley Pub. Co., Inc., c.1961.

2. Hogge, John E.: Three Ballistic Camera Data Reduction Methods Applicable to Reentry Experiments. NASA TN D-4260, 1967.

3. Becvar, A.: Skalnate Pleso Atlas of the Heavens 1950.0. Sky Pub. Corp., 1958.

4. Boss, Benjamin: General Catalogue of 33342 Stars for the Epoch 1950. Publ. No. 468, vol. III, Carnegie Inst. of Washington, 1937.

5. Nassau, Jason John: Practical Astronomy. Second ed., McGraw-Hill Book Co., Inc., 1948.

6. Anon.: The Air Almanac. U.S. Nav. Observ., May-Aug. 1967.

7. Jacchia, Luigi G.: Photographic Meteor Phenomena and Theory. Tech. Rep. No. Three (Contracts NOrd 8555 and 10455), Harvard Coll. Observ. and Center Anal., Massachusetts Inst. Technol., 1949.

8. Ayers, Wendell G.: Luminous Efficiency of an Artificial Meteor at 11.9 Kilometers Per Second. NASA TN D-2931, 1965.

9. Hamilton, J. F.: Reciprocity-Law Failure. The Theory of the Photographic Process, Third ed., T. H. James, ed., Macmillan Co., c.1966, pp. 132-143.